

Photon-number-resolving detection at $1.04\ \mu\text{m}$ via coincidence frequency upconversion

Kun Huang,¹ Xiaorong Gu,¹ Min Ren,¹ Yi Jian,¹ Haifeng Pan,¹ Guang Wu,¹ E Wu,^{1,2} and Heping Zeng^{1,3}

¹State Key Laboratory of Precision Spectroscopy, East China Normal University, Shanghai 200062, China

²e-mail: ewu@phy.ecnu.edu.cn

³e-mail: hpzeng@phy.ecnu.edu.cn

Received March 8, 2011; revised March 31, 2011; accepted April 10, 2011;
posted April 11, 2011 (Doc. ID 143823); published April 29, 2011

We demonstrate photon-number-resolving detection based on coincidence frequency upconversion. Pumped by synchronized pulses, the photon signal of the coherent state at $1.04\ \mu\text{m}$ was upconverted into visible replicas with preserved photon number distribution. The upconverted photons were then registered by a silicon multipixel photon counter. The photon-number-resolving performance was improved by reducing the background counts with a synchronous pump as the coincidence gate and reducing the intrinsic parametric fluorescence influence with long-wavelength pumping. A total detection efficiency of 3.7% was achieved with a quite low noise probability per pulse of 0.0002. © 2011 Optical Society of America

OCIS codes: 190.7220, 040.0040, 040.3060.

Photon-number-resolving detection (PNRD) supports promising and important applications in low-light-level detection, nonclassical photon statistics measurements, fundamental quantum optics experiments, and practical quantum information processing [1–3]. Typically, visible-light PNRD could be achieved with quite high quantum efficiency and low dark counts by using a silicon multipixel photon counter (Si-MPPC) [3,4]. At telecom wavelengths, PNRD could be reached with the so-called self-differencing technique applied on InGaAs-based avalanche photodiodes (APDs)[5]. It is nevertheless a challenge to directly measure photon number distribution at wavelengths around $1\ \mu\text{m}$ due to the insensitivity of silicon or InGaAs detectors at those wavelengths. Recent progress in frequency upconversion of quantum states has shown that IR photons could be detected efficiently [6–9] and that PNRD at IR wavelengths could be implemented by counting frequency-upconverted replicas in the visible regime. PNRD was demonstrated at $1559\ \text{nm}$ with a total detection efficiency of 4% and noise probability of 0.023 per pulse [10]. Such frequency-upconversion PNRD should, in principle, be applicable at wavelengths around $1\ \mu\text{m}$ for robust low-light-level detection and multiphoton state analysis.

Here we demonstrate PNRD at $1.04\ \mu\text{m}$ based on frequency upconversion pumped by synchronized pulses at $1.55\ \mu\text{m}$. The PNRD performance was improved by reducing the background noise with coincidence frequency upconversion, where the signal photons were located in the time window of the synchronized pump pulses, while the intrinsic nonlinear parametric fluorescence noise was dramatically reduced using the long-wavelength pump scheme. In the experiment, the coincidence frequency upconversion was performed in a periodically poled lithium niobate (PPLN) crystal, and the upconverted visible photons were detected by a Si-MPPC. With a quite low noise probability per pulse of 0.0002, the Poissonian distribution of the upconverted photons was observed directly.

As shown in Fig. 1, the whole system used in our experiment was composed of three parts: signal source, pump source, and upconversion detection. The signal

and pump sources were taken from two synchronized fiber lasers, which were arranged in the master–slave cavity configuration. The master was a mode-locking ytterbium-doped fiber laser (YDFL) operating at $3.565\ \text{MHz}$. In order to get a narrow spectrum to satisfy the quasi-phase-matching bandwidth ($0.3\ \text{nm}$) of PPLN crystal, a fiber Bragg grating (FBG) was inserted at the output of the YDFL [11,12]. The FBG reflection was taken as the signal source, and its spectrum was centered at $1.04\ \mu\text{m}$, with a FWHM bandwidth of $0.3\ \text{nm}$. The corresponding pulse duration was measured to be $6\ \text{ps}$ from the autocorrelation trace. The FBG transmission was amplified by an ytterbium-doped fiber amplifier before being injected into an erbium-doped fiber laser (EDFL) to achieve synchronous mode locking by means of the cross-phase modulation effect. In order to obtain an appropriate narrow spectrum of EDFL, a fiber bandpass filter with a $3\ \text{nm}$ bandwidth was employed in the laser cavity. The output of the EDFL was then amplified by a dual-stage erbium-doped fiber amplifier to the power of $64.8\ \text{mW}$ as the pump source. The spectrum of the pump source was centered at $1.55\ \mu\text{m}$, with an FWHM of $0.2\ \text{nm}$. The corresponding pulse duration was deduced to be

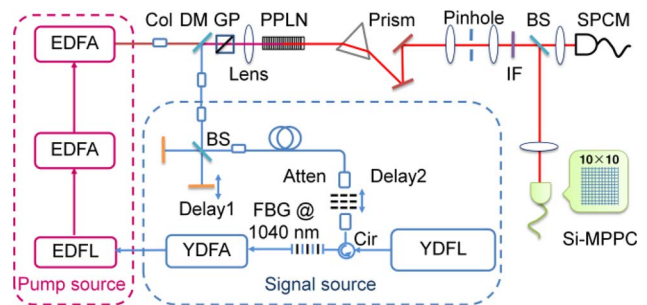


Fig. 1. (Color online) Experimental setup for the photon-number-resolved detection at $1.04\ \mu\text{m}$. Cir, circulator; Col, collimator; BS, beam splitter; DM, dichroic mirror; IF, interference filter; GP, Glan prism; Atten, attenuator; Si-MPPC, silicon multipixel photon counter; SPCM, single-photon counting module; YDFL, ytterbium-doped fiber laser; YDFA, ytterbium-doped fiber amplifier; EDFA, erbium-doped fiber amplifier; EDFL, erbium-doped fiber laser.

23 ps from the autocorrelation trace. The pulse duration of the pump was engineered to be longer than that of the signal, so that the pump pulses could be synchronously adjusted to envelop the signal pulses to improve the conversion efficiency [12,13]. For such passive synchronization of picosecond pulses, the timing jitter was normally about tens of femtoseconds [12], imposing a negligible influence on the temporal distribution of the signal photons within the pump pulse window.

The attenuated signal pulses at $1.04\ \mu\text{m}$ were then combined with the synchronized pump pulses by a dichroic mirror into a 50 mm long PPLN crystal. The operation temperature was set around $100.4\ ^\circ\text{C}$ with a fluctuation of less than $0.1\ ^\circ\text{C}$, which allowed a quasi-phase-matching frequency upconversion for the PPLN, with a grating period of $11.0\ \mu\text{m}$. The upconverted photons were steered through a group of filters with a transmittance η_F of 48.4% and then reflected by a beam splitter with a reflectance η_{BS} of 34.5% before focusing into a Si-MPPC with a multimode fiber input. The transmission from the beam splitter impinged into a conventional Si-APD single-photon counting module (SPCM) as a direct comparison. The Si-MPPC (Hamamatsu Photonics S10362-11-100U) was comprised of 10×10 APD pixels on an effective active area of $1\ \text{mm}^2$, with a photon detection efficiency η_D of 16.0%. When the incident photons were impinged into different APD pixels, the output voltage amplitude of the superposition from all pixels was proportional to the number of incident photons [3,4]. In order to minimize the thermal noise, the detector was Peltier cooled to $-35.0\ ^\circ\text{C}$. The breakdown voltage was set at 68.9 V, which was a compromise between the dark counts, quantum efficiency, and photon number resolution. The waveforms of the output voltage from the Si-MPPC were acquired for 2.81 ms by a digital oscilloscope. The recorded signal voltage was then postprocessed with a sampling gate of 32 ns to capture the photon clicks. The typical histogram of peak voltage shown in Fig. 2(a) was fitted by a series of Gaussian functions representing the different photon number state detections. The area of each peak was normalized by the total area to give the probability distribution shown in the inset of Fig. 2(a). As the input light was in a coherent state, the upconverted photons obeyed Poissonian statistics. By fitting the experimental data according to Poisson distribution, we got the detected photon number per pulse of 3.19 ± 0.01 . The error might

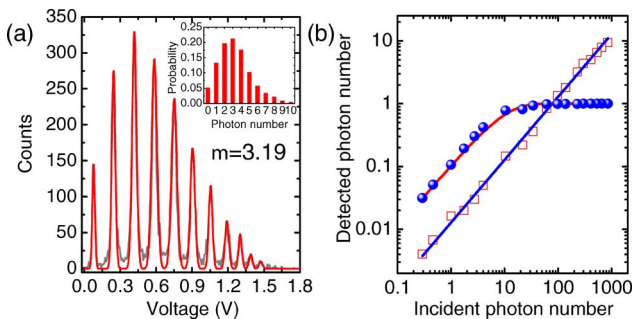


Fig. 2. (Color online) (a) Output voltage amplitude histogram for the upconverted photons. The photon number distribution is shown in the inset. (b) Detected photon numbers by SPCM (circles) and Si-MPPC (squares) as a function of incident photon numbers. Solid curves are the fits to the data.

be ascribed to the cross talk between adjacent APD pixels in the MPPC [4]. With the increase of the incident average photon number, the probability of detecting photons in successive pulses could not be negligible, which would result in insufficient charging of the detector for the second detection. Therefore, the corresponding avalanche amplitude would be smaller than the typical value, causing the slight mismatch of the fitting to the voltage amplitude histogram in the valleys in Fig. 2(a). Thanks to the pulsed pump in the upconversion system, the background noise induced by the strong pump was effectively reduced. Additionally, since the wavelength of the pump source was chosen to be longer than the signal, the noise from the pump-induced parametric fluorescence was efficiently suppressed [11,12]. Therefore, a quite low noise probability per pulse of 0.0002 was obtained in the experiment. Without the strong pump field, the background noise probability remained the same, indicating that the background noise was due to the intrinsic dark noise of the Si-MPPC itself and the stray background noise; thus, the parametric fluorescence noise in the upconversion process produced a negligible effect on the detection system. Such a low background noise probability could remarkably improve the sensitivity of the frequency-upconversion PNRD. The remarkable decrease in background noise would facilitate quantum optics experiments to directly demonstrate nonclassicality via photon counting [2,3].

With different average incident photon numbers, the photon numbers detected by SPCM were shown with circles in Fig. 2(b). Since SPCM could not discriminate more than one photon per shot, it was obviously saturated with large incident photon numbers. In contrast, as shown with squares in Fig. 2(b), the detected photon numbers of Si-MPPC linearly increased with the incident photon numbers. It showed that the Si-MPPC could correctly identify the photon numbers per pulse with a large dynamic range, which was promising in low-light-level detection. For inferring the total detection efficiency η_A of the frequency-upconversion PNRD, the experimental data were fitted by a solid curve with a slope of 1.28%. As the beam splitter in the experiment was employed for providing a direct comparison, it could be removed in practical applications. After taking into account the

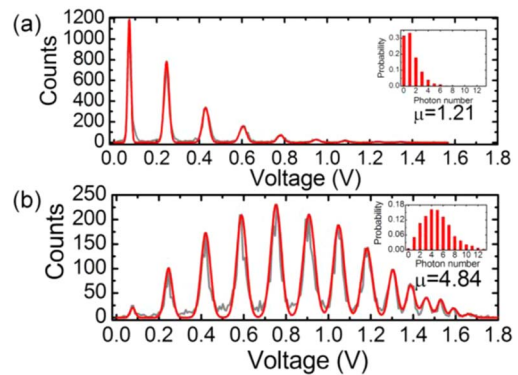


Fig. 3. (Color online) Output voltage amplitude histograms of frequency-upconversion PNRD (a) with one arm of the interferometer blocked and (b) with constructive interference. The corresponding photon number distributions are shown in the insets.

loss of the beam splitter, the total detection efficiency of the frequency-upconversion PNRD could be corrected to be 3.7% with η_A/η_{BS} . By correcting the overall efficiency for the measured optical losses with $\eta_A = \eta_C \times \eta_F \times \eta_{BS} \times \eta_D$, the conversion efficiency η_C could be inferred to be 47.9%. The limiting factor on the conversion efficiency would lie in the temporal aberrance of signal pulses because of the complicated mechanism of pulse formation and pulse evolution in an all-normal-dispersion YDFL operating at a low repetition rate [14]. Consequently, some signal photons were distributed outside the center of synchronized pump pulses, which resulted in the imperfect conversion efficiency. Thanks to recent advances in intracavity dispersion management, the pulse quality would be optimized to increase the conversion efficiency, thus increasing the total detection efficiency of the frequency-upconversion PNRD.

For further demonstration of its competence, a frequency-upconversion PNRD was used after a Michelson interferometer to monitor the intensity modulation of the signal source at $1.04\ \mu\text{m}$. As shown in Fig. 3, the photon numbers at the output of the Michelson interferometer were measured to be 1.21 with one arm blocked and 4.84 with constructive interference. The ratio of the photon numbers was 1/4, in accordance with the quantum optics theory of interference in a Michelson interferometer. It indicated that the photon numbers at $1.04\ \mu\text{m}$ could be correctly identified by the PNRD based on coincident frequency upconversion.

In summary, we have demonstrated PNRD at $1.04\ \mu\text{m}$ by photon-number-preserved frequency upconversion of single-photon pulses synchronously pumped by long-wavelength pulses and validated its competence by resolving photon number interference in a Michelson interferometer. Because of the pulsed radiation in the synchronization pumping system, much lower background noise than that in the continuous-wave pumping scheme was obtained, which would optimize applications such as quantum entanglement distribution and quantum teleportation [15] and improve the signal-to-noise ratio of widely used light detection and ranging systems. The approach may find promising applications in various quantum optics experiments using nonclassical light sources to demonstrate the nonclassicality of quantum states around $1\ \mu\text{m}$ [16,17].

This work was funded in part by the National Natural Science Fund of China (NSFC) (10990101, 60807027, 60907043, and 91021014), a Key project sponsored by the National Education Ministry of China (109069), the Research Fund for the Doctoral Program of Higher Education of China (200802691032), and the Innovation Program of Shanghai Municipal Education Commission (09ZZ47).

References

1. A. Allevi, M. Bondani, and A. Andreoni, *Opt. Lett.* **35**, 1707 (2010).
2. E. Waks, E. Diamanti, B. C. Sanders, S. D. Bartlett, and Y. Yamamoto, *Phys. Rev. Lett.* **92**, 113602 (2004).
3. I. Afec, A. Natan, O. Ambar, and Y. Silberberg, *Phys. Rev. A* **79**, 043830 (2009).
4. P. Eraerds, M. Legré, A. Rochas, H. Zbinden, and N. Gisin, *Opt. Express* **15**, 14539 (2007).
5. B. E. Kardynał, Z. L. Yuan, and A. J. Shields, *Nat. Photon.* **2**, 425 (2008).
6. S. Tanzilli, W. Tittel, M. Halder, O. Alibart, P. Baldi, N. Gisin, and H. Zbinden, *Nature* **437**, 116 (2005).
7. H. Takesue, E. Diamanti, C. Langrock, M. M. Fejer, and Y. Yamamoto, *Opt. Express* **14**, 13067 (2006).
8. M. T. Rakher, L. Ma, O. Slattery, X. Tang, and K. Srinivasan, *Nat. Photon.* **4**, 786 (2010).
9. M. A. Albota and F. N. C. Wong, *Opt. Lett.* **29**, 1449 (2004).
10. E. Pomarico, B. Sanguinetti, R. Thew, and H. Zbinden, *Opt. Express* **18**, 10750 (2010).
11. H. Dong, H. Pan, Y. Li, E. Wu, and H. Zeng, *Appl. Phys. Lett.* **93**, 071101 (2008).
12. K. Huang, X. Gu, H. Pan, E. Wu, and H. Zeng, "Synchronized fiber lasers for efficient coincidence single-photon frequency upconversion," *IEEE J. Sel. Topics Quantum Electron.*, doi: 10.1109/JSTQE.2010.2102005 (posted February 4, 2011, in press).
13. A. P. VanDevender and P. G. Kwiat, *J. Mod. Opt.* **51**, 1433 (2004).
14. A. Chong, W. H. Renninger, and F. W. Wise, *Opt. Lett.* **32**, 2408 (2007).
15. T. Honjo, H. Takesue, H. Kamada, Y. Nishida, O. Tadanaga, M. Asobe, and K. Inoue, *Opt. Express* **15**, 13957 (2007).
16. M. Vasilyev, S. Choi, P. Kumar, and G. M. D'Ariano, *Phys. Rev. Lett.* **84**, 2354 (2000).
17. M. Mehmet, H. Vahlbruch, N. Lastzka, K. Danzmann, and R. Schnabel, *Phys. Rev. A* **81**, 013814 (2010).